JOURNAL OF ADVANCED TRANSPORTATION
J. Adv. Transp. 2016; **50**:1506–1519
Published online 22 September 2016 in Wiley Online Library (wileyonlinelibrary.com). DOI: 10.1002/atr.1413

Model for the capacity of the urban signal intersection with work zone

Da Yang[1,2,3]*, Liling Zhu[1], Lina Ma[1] and Ruoxiao Sun[1]

[1]*School of Transportation and Logistics, Southwest Jiaotong University, Chengdu 610031, China*
[2]*Department of Computer Science and Engineering, The Hong Kong University of Science and Technology, Sai Kung, Hong Kong*
[3]*National United Engineering Laboratory of Integrated and Intelligent Transportation, Chengdu 610031, China*

SUMMARY

Work zones exist widely on urban arterials in the cities that are undergoing road construction or maintenance. However, the existing studies on arterial work zones are very limited, especially on the work zones at urban intersections, although they have a severe negative impact on the urban traffic system. For the first time, this study focuses on how work zones reduce intersection capacity. A type of widely observed work zone, the straddling work zone that straddles on a road segment and an intersection, is studied. A linear regression model and a multiplicative model suggested by Highway Capacity Manual are proposed respectively to determine the saturation flow rate of the signal intersection with the straddling work zone. The data of 22 straddling work zones are collected and used to evaluate the performances of the proposed models. The results display that the linear regression model outperforms the multiplicative model suggested by Highway Capacity Manual. The study also reveals that reducing approach (or exit) lanes and the mixture of motor vehicles and non-motor vehicles (and pedestrians) can significantly decrease the capacity of the intersection with straddling work zone. Therefore, in setting a straddling work zone, workers should try to ensure that the intersection approach and exit are unobstructed and set a separation for non-motors and pedestrians to avoid mixed traffic flow. Copyright © 2016 John Wiley & Sons, Ltd.

KEY WORDS: signal intersection; straddling work zone; capacity; model; impact factors

1. INTRODUCTION

In recent years, developed countries are maintaining and reconstructing aged traffic facilities and developing countries are constructing more new traffic facilities, which both bring a large number of work zones on city arterials and freeways. Work zones can disrupt the normal traffic flow and cause many traffic problems [1–5]. Studies have displayed that work zones can reduce road capacity [6–9] and increase traffic delay and traffic accident [1, 10–15]. Due to the wide existence of work zones in the world and the severe problems caused by work zones, many methods have been presented to reduce the negative effect of work zones on traffic.

This paper focuses on the capacity reduction problem caused by work zones. So far, numerous studies [6–9, 16–23] have been conducted to investigate how work zones impact highway capacity, and some models have been proposed to reflect the capacity variation for various work zone and traffic characteristics. The studies displayed that the following factors had a significant influence on the work zone capacity, work intensity [8, 19, 20, 24], heavy vehicle percentage [8, 18, 20–22, 24], distance of freeway entrance or exit to work zone [8], number of closed lanes [18–21, 24], location of closed lanes [19, 21, 24], lateral clearance [16, 24], work zone size [20, 24], work zone duration [18, 20, 21], and road grade [20, 21]. Different types of algorithm were also proposed to model the work zone capacity,

*Correspondence to: Da Yang, School of Transportation and Logistics, Southwest Jiaotong University, Chengdu 610031, China. E-mail: yangd8@swjtu.edu.cn

Copyright © 2016 John Wiley & Sons, Ltd.

including Highway Capacity Manual (HCM)-based models [6, 8, 22, 23], regression models [9, 18, 24, 25], and neural network-based models [7, 21].

However, the majority of the existing studies on the work zone capacity only focused on the freeway work zones, and the studies on work zones on urban arterials are very limited, especially on urban intersections [26]. The characteristics of the urban arterial work zone and the freeway work zone are significantly different, such as the traffic flow characteristics, capacity impact factors, work zone characteristic, and so on. The research results of the freeway work zone cannot be applied directly on the urban arterial work zone. To the best of our knowledge, only a couple of papers and reports investigated the problems of work zones on urban arteries. The report [27] qualitatively suggested several methods of improving the signal design of an intersection with work zone, such as adjusting the signal phasing and timing, shortening cycle lengths, and accommodation of pedestrians. However, the suggested methods lacked real data support and scientific analysis. Li and Bai [28] studied the crashes in highway work zones and found that the number of crashes happening at intersections was much less than the number of crashes happening at non-intersections, which may attribute to vehicles' relative lower speed at intersections. Shaaban and Elnashar [26] discussed the problem of the intersections with work zone and presented a work zone layout strategy at an intersection. Heaslip *et al*. [29] used the simulation method to estimate the capacity of work zones on arterial segments considering various factors, including the per cent of left turning vehicles, the distance from the work zone to the intersection, and the EG/C (effective green to cycle length) of each lane group. However, they did not explore the capacity problem of the work zone at an intersection.

In summary, no studies have investigated how work zones impact the intersection capacity yet, and no field data were mentioned too. This situation may attribute to the difficulties of collecting field data due to the limited number of work zones in many countries and too many complex factors involved in an urban road, such as the interference from pedestrians and non-motor vehicles, the location of a work zone at an intersection, etc. Fortunately, in recent years, China is undergoing a new period of traffic facility construction (especially the urban railway construction). Currently, in many cities of China, a large number of work zones exist on road segments and intersections, which provide the authors a valuable opportunity to observe and study the relationship of road capacity and work zones in cities. In this paper, for the first time, the authors collected the field data of 22 urban intersections with work zones in Chengdu, China, explored the factors that may have a significant impact on the intersection capacity, and further modeled the relationship of the intersection capacity and work zone characteristics.

Before this study, by observing many urban intersections with work zones, we classified the work zone at the urban signal intersection into two categories: the straddling work zone and the island work zone, respectively (Figure 1). The straddling work zone refers to the work zone that straddles the urban intersection and the road segment (Figure 1a). The island work zone refers to the work zone that is located within the area of the intersection (Figure 1b). Because these two types of work zone have different obvious characteristics, they will be studied separately in different papers.

This paper only focuses on the urban intersection with straddling work zone. The straddling work zones cause many driving conflicts owing to the two reasons. First, the traffic space at the intersections

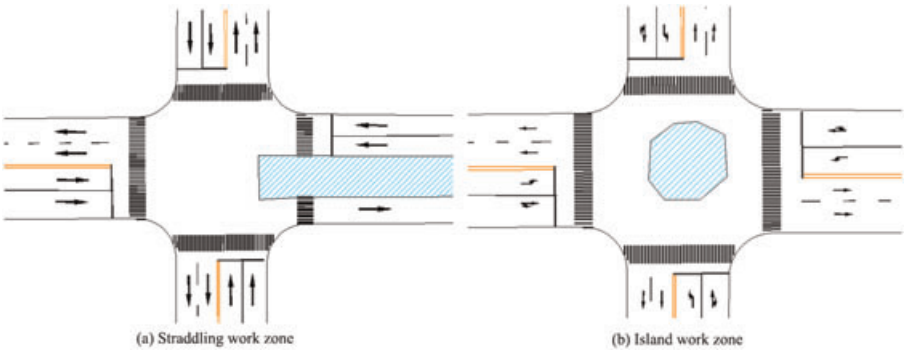


Figure 1. Two types of work zone related to urban intersections. (a) Straddling work zone; (b) island work zone.

Copyright © 2016 John Wiley & Sons, Ltd.

DOI: 10.1002/atr

is compressed by the straddling work zones, so there is not enough passing space for vehicles and pedestrians. Second, the pavements for non-motor vehicles and pedestrians are occupied, which causes heavy interactions between motor vehicles and non-motor vehicles (or pedestrians). Accordingly, the intersection traffic capacity will be reduced significantly. A work zone may affect the capacities of all the directions of an intersection. It should be noted that this paper only investigates the capacity of the direction from south to north in Figure 1a (the work zone side of the intersection), due to the word limitation.

The remainder of the paper is organized as follows: Section 2 presents the used data in this study. Section 3 proposes two models for the capacity of the intersection with straddling work zone. Section 4 evaluates the proposed models, and Section 5 concludes the paper and discusses the limitation of the study.

2. DATA INTRODUCTION

2.1. Factors influencing the capacity of the intersection with straddling work zone

Before data collection, the possible factors influencing the capacity of the straddling work zones are analyzed, which will help us to confirm what information needs to be collected. Based on numerous observations, it was found that the following factors may cause reduction of the capacity of the intersection with straddling work zone: heavy vehicles, work zone size stretched into the intersection, interference of non-motor vehicles and pedestrians, setting the separation for non-motor vehicles and pedestrians, and changes of the numbers of approach and exit lanes. Some early well-understood factors, such as the lane width, the percentage of left-turn vehicles (PLT), and the percentage of right-turn vehicles (PRT), are not explained here.

2.1.1. Heavy vehicles

Heavy vehicles have the characteristics of large size, occupying bigger road area, and moving slowly, so the presence of heavy vehicles at an intersection seriously influences the normal traffic operation. A work zone will decrease the passing space of the intersection, which may produce an extreme condition that the intersection only allows one heavy vehicle to pass and all the following cars are blocked by the heavy vehicle. Different from the situation on freeways, heavy vehicles in cities include two types: the bus and the truck. Buses are the main component of heavy vehicles in the intersection traffic flow, but a small number of trucks serving for the road construction also may exit.

2.1.2. Length and width of the work zone stretched into the intersection

At an intersection with straddling work zone, due to the presence of work zone, the traffic flow pattern is changed, as shown in Figure 2. At such an intersection, vehicles traveling from south to north have

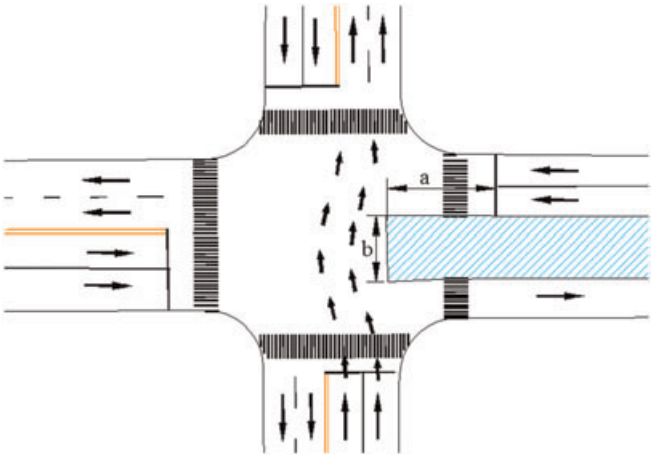


Figure 2. Traffic flow pattern of the intersection with straddling work zone.

Copyright © 2016 John Wiley & Sons, Ltd.

DOI: 10.1002/atr

to deviate from the original track that was blocked by the work zone and move to the central area of the intersection in Figure 2. This pattern change not only increases the distance for vehicles to pass through the intersection but also enhances the interaction of the traffic streams from the two directions, which may greatly cut down the intersection capacity. The increment of the size of the work zone stretched into the intersection will make the situation more severe. In Figure 2, a is the length of the work zone stretched into the intersection, and it is referred as the distance from the edge of the work zone to the stopping line of the intersection. b is the width of the work zone stretched into the intersection.

2.1.3. Pedestrians and non-motor vehicles

Another factor that may have a significant impact on the capacity of an intersection with straddling work zone is the number of pedestrians and non-motor vehicles. In some countries, such as China and India, there are a large number of pedestrians and non-motor vehicle users (electric bicycles or manpower bicycles). Generally, an intersection should provide pavements for pedestrians and non-motor vehicles, but a straddling work zone occupies the pavement and forces pedestrians and non-motor vehicles to enter into the space designed for motor vehicles, thereby producing a mixed traffic flow of pedestrians, non-motor vehicles, and motor vehicles, as shown in Figure 3. Due to the safety consideration, motor vehicles have to avoid pedestrians and non-motor vehicles, which will reduce the capacity of the intersection, and the reduction effect will increase with the increment of the number of pedestrians and non-motor vehicles.

2.1.4. Setting a separation for non-motor vehicles and pedestrians

At some intersections with straddling work zones, barriers are set up to separate non-motor vehicles and pedestrians from the motor vehicles, as shown in Figure 4, but not all intersections have such barriers. The barriers can protect the pedestrians and non-motor vehicles from directly conflicting with motor vehicles; on the other hand, they may regularize the behavior of pedestrians and non-motor drivers and make them walk or drive behind the separation, which will reduce conflicts with motor vehicles and further increase intersection capacity.

2.1.5. Number difference of approach lanes and exit lanes

It is widely known that the number of vehicles passing through the intersection in the green time is mainly determined by numbers of approach lanes and exit lanes [30]. At a normal intersection, the number of the approach lanes and the number of the exit lanes are balanced, while at many intersections with straddling work zones, the approach and exit have different lane numbers due to the construction work. The situation that the number of approach lanes (NAL) is less than the number of exit lanes (NEL) is widely observed at the intersections with straddling work zones, which seems to reduce the passing efficiency and capacity and form queues at the intersection.

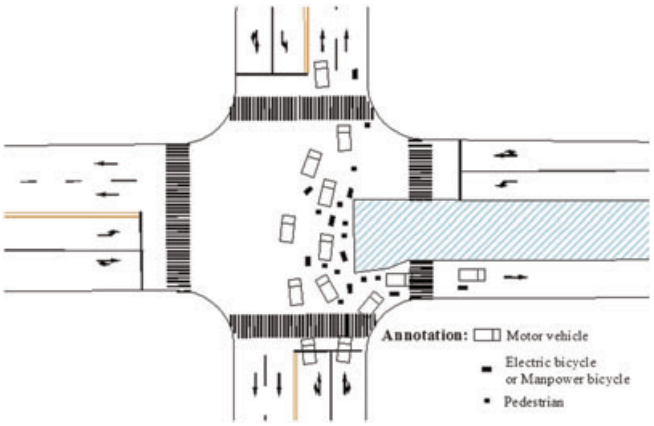


Figure 3. Mixed traffic at the intersection with straddling work zone.

Copyright © 2016 John Wiley & Sons, Ltd.

DOI: 10.1002/atr

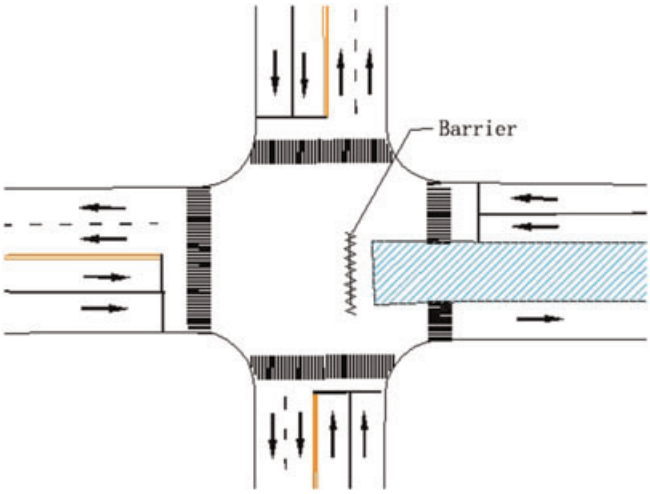


Figure 4. The separation for non-motor vehicles and pedestrians at an intersection.

2.2. Data collection

Because one of the metropolises of China, Chengdu, is undergoing a new period of traffic facility construction, especially the urban railway construction, work zones exist widely in the city, which gives the authors a valuable opportunity to observe and investigate how work zones impact the urban intersection capacity. Twenty-two intersections with straddling work zones were chosen. All the 22 work zones belonged to long-term construction, and their durations were more than half a year. The data collection time was the afternoon peak hour that was 5:30–6:30 PM. The data collection tools were video cameras. Although the cameras recorded the traffic data for all the directions of each intersection, this study only needs the traffic data from south to north in Figure 2. The recording duration of each intersection was over five cycles, and the final capacity was the average capacity values of the five cycles. After counting and calculation, the signal data and average traffic volume data of the 22 intersections with straddling work zone for a single period are displayed in Table I. Because the traffic volume is the average result of five cycles, some decimal numbers appear for vehicles. The traffic volume data in Table I present the volume of left-turn through right-turn of cars, buses, articulated buses, non-motor vehicles, and pedestrians in the effective green time. The signal information includes the cycle length (T), green time (G), yellow time (Y), red time (R), and effective green time (EG).

This study does not focus on shared lane group, so all the 22 chosen intersections only have exclusive through lane group or the study only use the through vehicle data. However, at an intersection with straddling work zone, due to the reduction of passing space, exclusive through lanes generally accommodate more left/right-turn vehicles comparing with the intersections without work zones. That is the reason why many left/right turn vehicles appear in the "car" column for several sites, for example, site 22. The data in Table I are the average value for five cycles.

In addition to the traffic volume data and signal data, the following factors that may have a significant impact on intersection capacity are also recorded and shown in Table II, including *NAL*, width of the approach lane (*WAL*), *NEL*, width of the exit lane (*WEL*), setting a separation for non-motor vehicles and pedestrians (*BS*; if yes, $BS=1$, else, $BS=0$), width of the passing space for pedestrians and non-motor vehicles behind the separation (*SW*), work zone length (*WL*) and width (*WD*) stretched into the intersection, and number of non-motor vehicles and pedestrians passing through the intersection (*NNP*) in effective green time. Furthermore, the following variables are calculated: percentage of heavy vehicles (*PHV*), *PLT*, *PRT*, the number difference of approach lanes and exit lanes ($NDL = NAL - NEL$), and total width reduce of intersection approach and exit ($TWR = NAL \cdot WAL - NEL \cdot WEL$). Several factors that had been proved to have a significant influence on the capacity of freeway work zone are ignored, including the work intensity and activity (active or inactive), work time (day or night), and traffic control strategy. The reasons are as follows: To avoid interfering with normal traffic, all the studied work zones are completely enclosed with hedges and the drivers outside

Copyright © 2016 John Wiley & Sons, Ltd.

DOI: 10.1002/atr

Table I. Data of traffic volume for different types of vehicle and signal period.

	Traffic volume in effective green time (left-turn/through/right-turn)					Signal period timing (s)				
Sites	Car	Bus	Articulated bus	Non-motor vehicle	Pedestrian	T	G	Y	R	EG
1	0/20/2	0/2/0	0/0/0	4/16/1	1/9/3	150	79	3	68	45
2	0/32/5	0/1/0	0/0/0	2/18/5	1/26/3	170	70	3	97	65
3	0/38/0	0/1/0	0/0/0	1/13/3	3/10/2	160	65	3	92	60
4	0/20/2	0/1.5/1	0/0.5/0	5/24/5	4/6/10	160	65	3	92	65
5	0/5.5/0	0/1.5/0	0/0/0	5/30/15	4/18/4	145	82	3	60	38
6	0/27/3	0/3/0.5	0/0/0	5/38/8	4/9/5	145	82	3	60	65
7	0/81/0	0/3/0	0/0/0	12/15/0	4/4/0	150	103	3	44	70
8	0/43/13	0/2/0	0/0/0	14/38/9	7/9/7	150	103	3	44	63
9	1/30/0	0/1/0	0/0/0	4/35/3	3/31/3	155	71	3	81	45
10	4/15/0	0.3/1/0	0/1/0	1/5/0	1/10/0	105	47	3	55	23
11	5/11/4	0.2/2/0.5	0/0/0	6/10/5	5/7/5	130	52	3	75	42
12	9/20/5	0.2/0.3/0	0/0/0	7/9/7	7/6/8	130	52	3	75	43
13	0/36/5	0/4/0	0/0/0	2/15/2	4/9/1	130	72	3	55	41
14	3/15/4	1/1/1	0/0/0	1/4/1	3/6/2	150	45	3	102	30
15	4/17/5	0.3/1.5/0	0/0/0	3/23/6	4/10/5	150	45	3	102	30
16	7.5/81.5/2	1.5/2.5/0	0/0.5/0	3/16/5	1/12/2	175	96	3	76	78
17	4/8/0	0/0.5/0	0/0/0	3/20/2	3/9/3	135	35	3	97	30
18	0/7.5/3.5	0/1/0.5	0/0/0	2/23/3	2/14/5	135	35	3	97	33
19	0/47/4	0/4.5/0	0/0.5/0	5/42/4	6/26/6	157	88	3	66	72
20	1.5/34/3.5	0.5/2.5/0	0/0.5/0	3/17/4	4/9/4	134	59	3	72	36
21	0/53/0	0/1.5/0	0/0/0	5/14/2	4/20/5	144	100	3	41	40
22	0/96/21	0/2.5/1	0/0.5/0	10/25/9	6/30/7	205	113	3	89	94

Table II. Data of the considered impact factors.

Sites	*NAL/NEL* (lanes)	*WAL/WEL* (m)	*WL/WD* (m)	*PHV* (%)	*PLT/PRT* (%)	*NNP* (vehs)	*BS*	*SW`* (m)	*NDL* (lanes)	*TWR* (m)
1	1.5/2	3.1/3.1	10.5/4.5	15.4	0.0/1.7	600	1	1.25	−0.5	−1.60
2	2/3	3.0/3.2	3.2/14.9	5.1	0.0/12.8	932	0	0	−1.	−3.59
3	2/2	3.1/3.6	14.9/10.4	5.0	0.0/1.0	518	1	2	0	−1.16
4	1/2.5	4.4/3.6	1.3/2.5	22.8	0.0/14.0	675	1	2	−1.5	−4.54
5	1/2	3.3/3.2	21.5/12.4	35.3	0.0/0.0	1192	1	2.5	−1	−3.08
6	2/3	3.5/3.6	6.3/6.3	18.9	0.0/10.8	1241	0	0	−1	−3.80
7	3/3	3.8/3.1	6.7/4.2	6.9	0.0/0.0	456	1	1.2	0	2.03
8	3/3	3.0/3.3	14.7/6.3	6.7	0.0/21.7	1128	1	3	0	−0.95
9	3/3	3.3/3.0	6.3/9.4	6.1	3.0/0.0	1533	1	2	0	0.79
10	4/4	2.9/3.0	15.8/10.5	22.8	18.7/0.0	514	0	0	0	−0.63
11	2/3	3.3/3.7	17.1/2.9	21.3	21.3/19.7	471	0	0	−1	−4.43
12	3/2	3.6/3.6	8.1/9.4	2.9	26.9/14.3	415	0	0	1	3.48
13	4/3	3.0/3.8	3.8/25.3	16.3	0.0/10.2	665	1	1.5	1	0.63
14	3/3	3.1/3.0	16.5/2.5	21.4	17.9/21.4	240	0	0	0	0.32
15	3/3	3.0/3.2	3.2/17.6	14.6	18.7/20.3	792	0	0	0	−0.38
16	4/3	3.1/3.2	9.5/10.1	9.5	10.5/2.0	576	0	0	−1	2.76
17	2/2	2.9/3.2	20.3/16.5	7.7	30.8/0.0	773	0	0	0	−0.57
18	2/2	2.85/3.2	22.2/17.1	21.4	0.0/32.1	987	0	0	0	−0.63
19	3/3	2.85/3.0	3.7/7.0	17.1	0.0/6.5	1559	1	3.7	0	−0.38
20	4/4	2.95/3.2	3.5/6.7	16.1	5.4/7.5	699	1	2.85	0	−0.86
21	4/4	3.10/3.1	3.2/5.6	5.4	0.0/0.0	850	1	3.92	0	0.13
22	4/3	3.07/4.2	3.4/6.7	6.7	0.0/19.0	966	0	0	−1	−0.38

the work zone hedges even cannot see the construction work, so work intensity and activity (active or inactive) will have no impact on the intersection capacity. Moreover, the vehicles transporting construction materials or wastes mainly work at late nights, and no traffic control devices are set before the studied intersections, so the work time (day or night) and the control strategy factor do not need to be considered in this paper.

Copyright © 2016 John Wiley & Sons, Ltd.

DOI: 10.1002/atr

3. CAPACITY MODEL OF THE SIGNAL INTERSECTION WITH STRADDLING WORK ZONE

3.1. HCM capacity algorithm for signal intersection

Highway Capacity Manual introduced a signal intersection capacity algorithm [30] for the exclusive through lane group, and it had been widely used to calculate the urban signal intersection capacity [31–33]. The formula of the algorithm is as follows:

$$C = S \cdot (G/T) \tag{1}$$

where C denotes the capacity of the signal intersection (*pcu/h*), S denotes the saturation flow rate of the signal intersection, and T denotes the signal period.

Equation (1) displays that when the signal timing is fixed, the saturation flow rate is the only factor determining the intersection capacity. The saturation flow rate is defined as the maximum flow passed the intersection under the condition of full green time ($G/T = 1$). For a specific signal intersection, the saturation flow rate is an adjusted result determined by many factors, such as the PHV, WAL, and the percentage of turn vehicles. HCM also introduced a function to calculate the adjusted saturation flow rate as follows:

$$S = S_0 f_w f_{HV} f_g f_p f_{bb} f_a f_{RT} f_{LT} \tag{2}$$

where S_0 denotes the base saturation flow rate; and $f_w, f_{HV}, f_g, f_p, f_{bb}, f_a, f_{RT}$, and f_{LT} respectively denote the adjustment compensation coefficients for the lane width, heavy vehicle, approach grade, existence of a parking lane, and parking activity adjacent to lane drop, blocking effect of local buses stopping within intersection area, area type (business district equals 0.9, else equals 1.0), right-turn vehicle presence, and left-turn vehicle presence.

Taking advantage of Equations (1) and (2), the theoretical capacities (assume without work zones) of the 22 intersections are calculated. The data are summarized and shown in Table III. S_t denotes the theoretical saturation flow rate, C_t denotes the theoretical capacity calculated based on Equation (1) without considering the influence of work zones, and C_a denotes the actual average capacity of the intersection calculated by using the data in Table I. From Table III, it can be observed that the actual

Table III. Capacity data and saturation flow data.

Sites	S_t	C_t	C_a	$C_t - C_a$	$(C_t - C_a) \times 100 / C_t$
1	1387	1280	1109	171	13.4%
2	1098	1320	838	482	36.5%
3	1200	1430	990	440	30.8%
4	1578	713	651	62	8.7%
5	805	791	461	330	41.7%
6	1025	1617	1173	444	27.5%
7	1491	3882	3102	780	20.1%
8	1042	3008	2377	631	21.0%
9	880	2213	1226	987	44.6%
10	963	2822	1760	1062	37.6%
11	1089	1239	888	351	28.3%
12	977	2129	1195	934	43.9%
13	1076	3500	2416	1084	31.0%
14	1120	1383	1030	353	25.5%
15	984	1347	905	442	32.8%
16	1160	3717	2571	1146	30.8%
17	780	887	416	471	53.1%
18	764	670	407	263	39.3%
19	938	2563	1743	820	32.0%
20	1129	2800	2082	718	25.6%
21	1260	4878	3535	1343	27.5%
22	1211	3387	2694	693	20.5%

Copyright © 2016 John Wiley & Sons, Ltd.

DOI: 10.1002/atr

capacity values are significantly less than the theoretical values due to the presence of the straddling work zones. The worst case is site 17, where the capacity decreases more than half.

The comparisons mentioned in the preceding texts illustrate that the straddling work zones greatly decrease the capacities of the intersections, and it is necessary to analyze and model how work zones impact the intersection capacities.

3.2. Saturation flow rate models

3.2.1. Correlation analysis

Before modeling the relationship of the intersection capacity and the impact factors, the correlation analysis should be taken to find out the key factors in determining the capacity. To realize this purpose, the correlation coefficient r of the two groups of variable $X=(x_1, x_2, \dots, x_n)^T$ and $Y=(y_1, y_2, \dots, y_n)^T$ is calculated by using the following formula [34]:

$$r = \frac{n\sum_{i=1}^{n} x_i y_i - \sum_{i=1}^{n} x_i \sum_{i=1}^{n} y_i}{\sqrt{\left[n\sum_{i=1}^{n} x_i^2 - \left(\sum_{i=1}^{n} x_i\right)^2\right] \cdot \left[n\sum_{i=1}^{n} y_i^2 - \left(\sum_{i=1}^{n} y_i\right)^2\right]}} \tag{3}$$

where x denotes the independent variables, that is, the impact factors here; and y denotes the dependent variable, that is, the saturation flow rate of the intersection for each lane (S_a) here.

The correlation analysis results are displayed in Table IV. It can be observed that the four factors—*WAL*, *WEL*, *BS*, and *SW*—have negative correlation coefficient signs, which means that the intersection capacity will decrease with the increment of the values of the four factors. In contrast, the other eight factors—*WL*, *WD*, *PHV*, *PLT*, *PRT*, *NNP*, *NDL*, and *TWR*—have positive correlation coefficient signs, which indicates that the intersection capacity will increase with the increment of the values of the eight factors. In addition, the r value between *BS* and *SW* is 0.88, which indicates that they have great information overlapping, and the r value between *SW* and S_a is 0.18 that is less than the one between *BS* and S_a, so *SW* also will be excluded from the consideration in modeling.

3.2.2. Linear regression model

According to the results of statistics and correlation analysis, stepwise regression method [35] was used to select independent variables of the capacity model. Beforehand, the nine arguments (*WAL*, *WEL*, *WL*, *WD*, *PHV*, *PLT*, *NNP*, *BS*, and *NDL*) that have higher correlation value with S_a are chosen to establish a linear regression model to reflect the relationship of the impact factors and intersection capacities. The HCM capacity algorithm is still adopted in calculating the capacity, but the saturation

Table IV. Correlation analysis results.

	S_a	*WAL*	*WEL*	*WL*	*WD*	*PHV*	*PLT*	*PRT*	*NNP*	*BS*	*SW*	*NDL*	*TWR*
S_a	1.00												
WAL	0.59	1.00											
WEL	0.20	0.28	1.00										
WL	−0.49	−0.30	−0.19	1.00									
WD	−0.54	−0.42	0.06	0.09	1.00								
PHV	−0.15	0.08	−0.14	0.37	−0.01	1.00							
PLT	−0.36	−0.08	−0.06	0.33	0.09	−0.04	1.00						
PRT	−0.10	−0.04	0.27	0.09	0.03	0.15	0.05	1.00					
NNP	−0.43	−0.18	−0.14	−0.15	0.12	0.04	−0.46	−0.06	1.00				
BS	0.37	0.19	−0.15	−0.24	−0.16	0.00	−0.62	−0.42	0.26	1.00			
SW	0.18	0.01	−0.24	−0.25	−0.21	−0.01	−0.54	−0.35	0.42	0.88	1.00		
NDL	−0.32	−0.33	−0.14	0.03	0.41	−0.32	0.26	−0.04	−0.16	0.14	0.13	1.00	
TWR	−0.09	−0.19	−0.16	−0.09	0.17	−0.50	0.24	−0.18	−0.21	−0.02	−0.04	0.67	1.00

Copyright © 2016 John Wiley & Sons, Ltd.

DOI: 10.1002/atr

flow rate model will adopt the linear regression formula. In the linear regression model, the dependent variable is S and the independent variables are the nine factors. Thus, there is the following equation:

$$S = a_0 + \sum_i a_i z \tag{4}$$

where a_0 and a_i are the parameters and z denotes the nine selected impact factor.

However, after applying the field data to regress the proposed model, it is found that under the 90% confidence level, the p-value of *WEL* is 0.78, which is much bigger than the significance level (0.10), so the factor *WEL* is excluded from the independent variable list. We use the rest eight arguments to establish a regression analysis, and the regression result is significant. Moreover, we add the two variables—*PRT* and *TWR*—that also have a high correlation with S_a into the independent variable list, in which we found that the p-values of *PRT* and *TWR* are all much larger than the significance level. Thus, *PRT* and *TWR* are also excluded from the independent variable list. In the end, the formula of the proposed linear regression model is as follows:

$$S = a_0 + a_1 WAL + a_2 WL + a_3 WD + a_4 PHV + a_5 PLT + a_6 NNP + a_7 BS + a_8 NDL \tag{5}$$

where, a_0, a_1, a_2, a_3, a_4, a_5, a_6, a_7, and a_8 are the parameters need to be calibrated.

Table V displays the regression results of the proposed model by using the field data, including the parameter values, standard errors, t-Stat, and p-values of all the parameters. The p-values in Table V indicate that all the considered factors are significant in estimating the signal intersection capacity with straddling work zone in a confidence level of 90%. Therefore, according to the analysis mentioned in the preceding texts and the results in Table V, the final expression of the proposed model is as follows:

$$\begin{aligned} S = {} & 1337.9 + 77.3WAL – 9.7WL – 6.56WD – 3.17PHV – 6.32PLT – 0.41NNP \\ & + 110.2BS – 95.2NLR \end{aligned} \tag{6}$$

Equation (6) illustrates that *WAL* and *BS* are positive factors and *WL*, *WD*, *PHV*, *PLT*, *NNP*, and *NLR* are the negative factors in determining the capacity of the intersection with straddling work zone, which is consistent with the correlation analysis results and common intuitions. *WAL*, *BS*, and *NLR* are the three most sensitive factors, and the WZL is more sensitive than the work zone width. In the nine factors, *WAL* and *NLR* are the two factors concerning the intersection approach and exits and both of them have large coefficient values, which reveals that it is important to assure the approach and exit lanes are unobstructed in the layout of work zones. *BS* also has a large coefficient value, and in practice, it is easy to set a separation for non-motor vehicles and pedestrians, so engineers should set the separation and avoid the mixture of motors and non-motors (or pedestrians) at the intersection.

The goodness-of-fit and residual error of the proposed model are exhibited in Table VI. The *R-square* value indicates that the proposed model can reflect 96% of the relationship between the capacity and the eight chosen factors. All the statistical results support the conclusion that the proposed

Table V. Regression results.

Variable	Parameter values	Standard error	t-Stat	p-value
CON	1337.93	149.93	8.92	0.00
WAL	77.25	41.27	1.87	0.08
WL	−9.70	2.19	−4.43	0.00
WD	−6.56	2.55	−2.57	0.02
PHV	−3.17	1.71	−1.85	0.08
PLT	−6.32	1.89	−3.34	0.01
NNP	−0.41	0.04	−10.02	0.00
BS	110.22	36.77	3.00	0.01
NDL	−95.15	27.66	−3.44	0.00

Copyright © 2016 John Wiley & Sons, Ltd.

DOI: 10.1002/atr

Table VI. Goodness-of-fit and residual error of the model.

	Linear regression model
Multiple *R*	0.979
R-square	0.960
Adjusted *R*-square	0.932
Significance *F*	0.000

linear regression model has good performance and the eight factors are significant in determining the capacity.

3.2.3. HCM-based model

In addition to the linear regression model mentioned in the preceding texts, the authors also propose a multiplicative model to calculate the saturation flow rate, which follows the form given by HCM, named HCM-based model. The formula of the HCM-based model is as follows:

$$S = S_0 f_{\mathrm{WAL}} f_{\mathrm{WL}} f_{\mathrm{WD}} f_{\mathrm{PHV}} f_{\mathrm{PLT}} f_{\mathrm{PRT}} f_{\mathrm{NNP}} f_{\mathrm{SW}} f_{\mathrm{TWR}} f_{\mathrm{a}} \tag{7}$$

where f_{WAL}, f_{WL}, f_{WD}, f_{PHV}, f_{PLT}, f_{PRT}, f_{NNP}, f_{SW}, and f_{TWR} denote the compensation coefficients for the nine factors: *WAL*, *WL*, *WD*, *PHV*, *PLT*, *PRT*, *NNP*, *SW*, and *TWR*.

In Equation (7), the coefficients f_{WAL}, f_{PHV}, f_{PLT}, f_{PRT}, and f_{a} are five common factors for general intersections without work zones and their values can be found in the reference [36], but the other five coefficients f_{WL}, f_{WD}, f_{NNP}, f_{SW}, and f_{TWR} are new and need to be calculated. To make the estimation more accurate, the following forms of f_{WL}, f_{WD}, f_{NNP}, f_{SW}, and f_{TWR} are adopted:

$$f_{\mathrm{WL}} = wl_1 + wl_2 \cdot WL \tag{8}$$

$$f_{\mathrm{WD}} = wd_1 + wd_2 \cdot WD \tag{9}$$

$$f_{\mathrm{NNP}} = nnp_1 + nnp_2 \cdot NNP \tag{10}$$

$$f_{\mathrm{SW}} = sw_1 + sw_2 \cdot SW \tag{11}$$

$$f_{\mathrm{TWR}} = twr_1 + twr_2 \cdot TWR \tag{12}$$

where wl_1, wl_2, wd_1, wd_2, nnp_1, nnp_2, sw_1, sw_2, twr_1, and twr_2 are the parameters needed to be calibrated.

The calibration process of the parameters in Equations (8–12) is as follows: First, according to the correlation analysis, the sign of the parameters is analyzed and fixed. Taking the function of *WL* as an example, $f_{\mathrm{WL}} = wl_1 + wl_2 \cdot WL$, $f_{\mathrm{WL}} > 0$ and with the increment of *WL*, the value of f_{WL} decreases, so wl_1 should have a positive sign and wl_2 should have a negative sign. Second, the feasible ranges of the parameters are narrowed into a possible area. Still taking $f_{\mathrm{WL}} = wl_1 + wl_2 \cdot WL$ as an example, when *WL* equals 0, f_{WL} should be 1, so the value of wl_1 is taken as 1. In addition, the value of *WL* can be up to 22.2 m in our study and f_{WL} is less than 1, so to ensure $f_{\mathrm{WL}} > 0$, wl_2 should be more than -0.045. Therefore, the feasible range of wl_2 is $[-0.045, 0]$. Third, after the ranges of the model parameters are fixed, the models are calibrated by using genetic algorithm to find the optimal value. Applying the field data to calibrate the HCM-based saturation flow rate model, the values of the coefficients are obtained and displayed in Table VII. In the next section, the accuracy of the two models will be compared by using statistical indexes.

Copyright © 2016 John Wiley & Sons, Ltd.

DOI: 10.1002/atr

Table VII. Parameter values of HCM-based model.

Parameters	wl_1	wl_2	wd_1	wd_2	nnp_1	nnp_2	sw_1	sw_2	twr_1	twr_2
Values	1	−0.00005	1	−0.0014	1	−0.00016	0.524	0.128	1	−0.0582

4. MODEL PERFORMANCE EVALUATION

Figure 5 displays the estimated capacity values by using the two models presented in Section 3 for the 22 intersections. From Figure 5, we can observe that the linear regression model is more approximate to the surveyed data than the HCM-based model.

To further evaluate the performances of the two models, the following indexes are adopted: mean error (*ME*), mean absolute error (*MAE*), mean absolute percentage error (*MAPE*), and standard deviation error (*SDE*). Their equations are as follows,

$$ME = \frac{1}{M}\sum_{i=1}^{M}\left(S_i - \hat{S}_i\right) \tag{13}$$

$$MAE = \frac{1}{M}\sum_{i=1}^{M}\left|S_i - \hat{S}_i\right| \tag{14}$$

$$MAPE = \frac{100}{M}\sum_{i=1}^{M}\frac{\left|S_i - \hat{S}_i\right|}{S_i} \tag{15}$$

$$SDE = \sqrt{\frac{1}{M}\sum_{i=1}^{M}\left(\frac{\left|S_i - \hat{S}_i\right|}{S_i} - MAPE\right)} \tag{16}$$

where S_i denotes the actual saturation flow rate value of the ith site, $\hat{S}_i$ denotes the estimated saturation flow rate value of the ith site, and M denotes the number of sites, that is, 22 here.

The evaluation results are shown in Table VIII, which indicates that the proposed linear regression model exhibits better performance than the HCM-based model. Generally, the error of the HCM-based model is about five times of the linear regression model. Therefore, it is safe to say that the proposed linear regression model can be used to model the urban signal intersection capacity with straddling work zone.

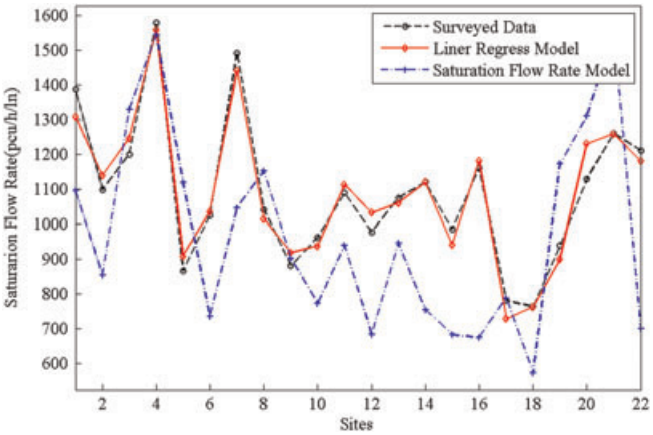


Figure 5. Comparison of actual and estimation values.

Copyright © 2016 John Wiley & Sons, Ltd.

DOI: 10.1002/atr

Table VIII. Error results of the two models.

	ME	*MAE*	*MAPE*	*SDE*
Linear regression model	0	50.31	4.9%	0.032
HCM-based model	122.6	234.27	21.4%	0.115
Difference percentage (%)	–	78.5%	77.1%	53.6%

5. CONCLUSION AND FUTURE WORK

The majority of the existing studies concerning the work zone capacity focused on the freeway work zones. The influence of work zones on the capacity of the urban arterials had not been explored carefully, especially on the urban intersections, due to the absence of field data. China is undergoing a new period of traffic facility construction, which provides us a valuable opportunity to observe and study the relationship between the urban arterial capacity and work zones. This paper focuses on modeling the capacity of the signal intersection with straddling work zone. For the first time, two models are proposed to estimate the saturation flow rate of the signal intersection with straddling work zone, the linear regression model and the multiplicative model following HCM's form, and the capacity data of the 22 intersections are collected. The factors that may have a significant influence on the capacity of the signal intersection with straddling work zone are discussed and analyzed by using correlation analysis method. The results reveal that the following factors are highly related to the intersection capacity: the width of approach lanes, width of exit lanes, WZL, work zone width, PHV, PLT, NNP, setting a separation for non-motor vehicles and pedestrians, and number difference of approach lanes and exit lanes. The performance of the two proposed models is evaluated, and the results exhibit that the linear regression model has acceptable errors and outperforms the HCM-based model. The linear regression model can be put forward to provide the necessary reference on urban traffic control, signal timing and work zone planning, and so on. In the aspect of practice, to increase the capacity of the intersection with straddling work zone, it is important to ensure that the approach and exit of the intersection are unobstructed when arranging a work zone within an intersection and engineers should set the separation for non-motor vehicles and pedestrians to avoid the occurrence of mixed flow.

However, this paper still has some limitations. First, due to the long construction terms of the subways (generally more than 2 years), we only collected the data of 22 work zones. In the future, more work zone data should be collected to validate our results further. Second, the paper only uses parametric models, but the non-parametric models that may have higher accuracy are not discussed here. Third, this paper only focuses on the straddling work zone, and the island work zone will be explored in the future too.

6. LIST OF SYMBOLS AND ABBREVIATIONS

T	cycle length
G	green time
Y	yellow time
R	red time
EG	effective green time
NAL	number of approach lanes
WAL	width of the approach lane
NEL	number of exit lanes
WEL	width of the exit lane
BS	whether setting a separation for non-motor vehicles and pedestrians
SW	width of the passing space for pedestrians and non-motor vehicles behind the separation
WL	work zone length
WD	work zone width

Copyright © 2016 John Wiley & Sons, Ltd.

DOI: 10.1002/atr

NNP	number of non-motor vehicles and pedestrians passing through the intersection
PHV	percentage of heavy vehicles
PLT	percentage of left-turn vehicles
PRT	percentage of right-turn vehicles
NDL	number difference of approach lanes and exit lanes
TWR	total width reduce of the intersection approach and exit
HCM	Highway Capacity Manual
C	capacity of the signal intersection
S	saturation flow rate of the signal intersection
S_0	base saturation flow rate
f_w	adjustment compensation coefficients for the lane width
f_{HV}	adjustment compensation coefficients for the heavy vehicle
f_g	adjustment compensation coefficients for the approach grade
f_p	existence of a parking lane and parking activity adjacent to lane drop
f_{bb}	blocking effect of local buses stopping within intersection area
f_a	area type
f_{RT}	right-turn vehicle presence
f_{LT}	left-turn vehicle presence
S_t	theoretical saturation flow rate
C_t	theoretical capacity
C_a	actual average capacity
r	correlation coefficient
x	independent variables in correlation analysis
y	dependent variables in correlation analysis
S_a	saturation flow rate of the intersection for each lane
z	selected 9 impact factors
f_{WAL}, f_{WL}, f_{WD}, f_{PHV}, f_{PLT}, f_{PRT}, f_{NNP}, f_{SW} and f_{TWR}	compensation coefficients for the 9 factors, WAL, WL, WD, PHV, PLT, PRT, NNP, SW and TWR
a_0, a_i, wl_1, wl_2, wd_1, wd_2, nnp_1, nnp_2, sw_1, sw_2, twr_1 and twr_2	the parameters appeared in the linear regression model
GA	Genetic Algorithm
ME	mean error
MAE	mean absolute error
MAPE	mean absolute percentage error
SDE	standard deviation error
S_i	actual saturation flow rate value of the i^{th} site
$\hat{S}_i$	estimated saturation flow rate value of the i^{th} site
M	number of the studied sites

ACKNOWLEDGEMENTS

This work was supported by the National Science Foundation of China (grant nos. 51278429 and 51408509) and the Fundamental Research Funds for the Central Universities (grant no. 2682016CX046).

REFERENCES

1. Weng J, Zhu J-Z, Yan X Liu Z. Investigation of work zone crash casualty patterns using association rules. *Accident Analysis & Prevention* 2016; **92**: 43–52.
2. Wang H, Liu L, Dong S, Qian Z Wei H. A novel work zone short-term vehicle-type specific traffic speed prediction model through the hybrid EMD–ARIMA framework. *Transportmetrica B: Transport Dynamics* 2015; 1–28.
3. Ying W., Qiao F., and Yu L. Evaluation of the impact of work zone on vehicular emissions in consideration of roughness profile. Presented at Transportation Research Board 95th Annual Meeting, 2016.

Copyright © 2016 John Wiley & Sons, Ltd.

DOI: 10.1002/atr

4. Sun C., Mackley A., and Edara P. Programmatic examination of Missouri incentive/disincentive contracts for mitigating work zone traffic impacts. *Journal of Construction Engineering and Management*, Vol.**140**, No.1, 2013, pp.04015064-1–04015064-9.
5. Weng J, Meng Q Yan X. Analysis of work zone rear-end crash risk for different vehicle-following patterns. *Accident Analysis & Prevention* 2014; **72**: 449–457.
6. Heaslip K., Kondyli A., Arguea D., Elefteriadou L., and Sullivan F. Estimation of freeway work zone capacity through simulation and field data. *Transportation Research Record: Journal of the Transportation Research Board*, Vol.**2130**, No.1, 2009, pp.16–24.
7. Karim A., and Adeli H. Radial basis function neural network for work zone capacity and queue estimation. *Journal of Transportation Engineering*, Vol.**129**, No.5, 2003, pp.494–503.
8. Krammes R. A., and Lopez G. O. Updated short-term freeway work zone lane closure capacity values. Transportation Research Record: *Journal of the Transportation Research Board*, Vol.**1442**, No.1, 1994, pp.49–56.
9. Weng J., and Yan X. New methodology to determine work zone capacity distribution. Transportation Research Record: *Journal of the Transportation Research Board*, No.2461, 2014, pp. 25–31.
10. Cassidy M. J., and Han L. D. Proposed model for predicting motorist delays at two-lane highway work zones. *Journal of Transportation Engineering*, Vol.**119**, No.1, 1993, pp.27–42.
11. Chitturi M., and Benekohal R. Work zone queue length and delay methodology. *Transportation Letters: the International Journal of Transportation Research*, Vol.**2**, No.4, 2010, pp.273–283.
12. Jiang X., and Adeli H. Freeway work zone traffic delay and cost optimization model. *Journal of Transportation Engineering*, Vol.**129**, No.3, 2003, pp.230–241.
13. Lawson T. W., Lovell D. J., and Daganzo C. F. Using input–output diagram to determine spatial and temporal extents of a queue upstream of a bottleneck. Transportation Research Record: *Journal of the Transportation Research Board*, Vol.**1572**, No.1, 1997, pp.140–147.
14. Khattak A. J., Khattak A. J., and Council F. M. Effects of work zone presence on injury and non-injury crashes. *Accident Analysis & Prevention*, Vol.**34**, No.1, 2002, pp.19–29.
15. Nemeth Z. A., and Rathi A. Freeway work zone accident characteristics. *Transportation Quarterly*, Vol.**37**, No.1, 1983, pp.145–159.
16. Yeom C., Hajbabaie A., Schroeder B. J., Vaughan C., Xuan X., and Rouphail N. M. Innovative work zone capacity models from nationwide field and archival sources. Transportation Research Record: *Journal of the Transportation Research Board*, No.2485, 2015, pp. 51–60.
17. Kim T., Lovell D. J., and Paracha J. A new methodology to estimate capacity for freeway work zones. Presented at Transportation Research Board Annual Meeting CD-ROM, 2001.
18. Weng J., and Yan X. Probability distribution-based model for work zone capacity prediction. *Journal of Advanced Transportation*, Vol.**50**, No.2, 2015, pp.165–179.
19. Dixon K. K., Hummer J. E., and Lorscheider A. R. Capacity for North Carolina freeway work zones. Transportation Research Record: *Journal of the Transportation Research Board*, Vol.**1529**, No.1, 1996, pp.27–34.
20. Jiang X., and Adeli H. Object-oriented model for freeway work zone capacity and queue delay estimation. *Computer-Aided Civil and Infrastructure Engineering*, Vol.**19**, No.2, 2004, pp.144–156.
21. Adeli H., and Jiang X. Neuro-fuzzy logic model for freeway work zone capacity estimation. *Journal of Transportation Engineering*, Vol.**129**, No.5, 2003, pp.484–493.
22. Al-Kaisy A., and Hall F. Guidelines for estimating capacity at freeway reconstruction zones. *Journal of Transportation Engineering*, Vol.**129**, No.5, 2003, pp.572–577.
23. Edara P., Kianfar J., and Sun C. Analytical methods for deriving work zone capacities from field data. *Journal of Transportation Engineering*, Vol.**138**, No.6, 2012, pp.809–818.
24. Kim T, Lovell DJ Paracha J. *A New Methodology to Estimate Capacity for Freeway Work Zones*Presented at Proceedings of the Annual Meeting of the Transportation Research Board: CDROM, 2001.
25. Memmott JL, Dudek CL. *Queue and User Cost Evaluation of Work Zones (QUEWZ)*1984.
26. Shaaban K., and Elnashar D. Evaluation of work zone strategies at signalized intersections. *Journal of Traffic and Logistics Engineering*, Vol.**1**, No.2, 2013, pp.202–206.
27. NYSDT. Highway design manual in highway work zones. 2006.
28. Li Y., and Bai Y. Fatal and injury crash characteristics in highway work zones. Presented at Transportation Research Board 87 th Annual Meeting, 2006.
29. Heaslip K., Jain M., and Elefteriadou L. Estimation of arterial work zone capacity using simulation. *Transportation Letters*, Vol.**3**, No.2, 2011, pp.123–134.
30. TRB. Highway Capacity Manual. 2010.
31. Akcelik R. *Traffic Signals: Capacity and Timing Analysis*ARRB Group Limited: Vermont South, Victoria, 1981.
32. Luttinen RT, Nevala R. *Capacity and Level of Service of Finnish Signalised Intersections*ARRB Group Limited: Vermont South, Victoria, 2002.
33. Teply S, Allingham D, Richardson D Stephenson B. *Canadian Capacity Guide for Signalized Intersections* (3rd edn)Ottawa: Institute of Transportation Engineering, 2008.
34. Ezekiel M. *Methods of Correlation Analysis*Wiley: Oxford, England, 1930.
35. Huang C., and Townshend J. A stepwise regression tree for nonlinear approximation: applications to estimating subpixel land cover. *International Journal of Remote Sensing*, Vol.**24**, No.1, 2003, pp.75–90.
36. Roess R. P., Prassas E. S., and McShane W. R.: Traffic engineering. Pearson/Prentice Hall. Englewood Cliffs, NJ 07632 USA, 2004.

Copyright © 2016 John Wiley & Sons, Ltd.

DOI: 10.1002/atr